Sh and Eag K^+ Channel Subunit Interaction in Frog Oocytes Depends on Level and Time of Expression

Mai-Lei Chen,* Toshinori Hoshi,† and Chun-Fang Wu*
Departments of *Biological Sciences and †Physiology and Biophysics, The University of Iowa, Iowa City, Iowa 52242 USA

ABSTRACT Subcellular clustering of ion channels critically affects neuronal function. Coexpression of Eag and Sh channel subunits in *Xenopus* oocytes leads to accelerated decay of the Sh-like transient K^+ current (Chen, M.-L., T. Hoshi, and C.-F. Wu. 1996. *Neuron.* 17:535–542). We report that such interaction depends critically on functional expression level (controlled by RNA injection quantities and indicated by current amplitudes) and developmental time after RNA injection. The accelerated decay became apparent 3 days after coinjection and increased thereafter. This was observed in different ionic conditions and at different voltage steps. However, decay was not accelerated at low expression levels, either within 1–2 days after injection or with reduced amounts of RNA. With sequential RNA injection, preformation of either Eag or Sh channels prevented interactions with the other subunit. The carboxyl terminus of Eag was found to be involved in accelerating, and in retarding recovery from, N-type inactivation. The interaction was reduced upon patch excision in macropatch measurements, suggesting involvement of cytosolic factors. We have reproduced the absence of interaction between Eag and Sh reported previously within 2 days after RNA injection and with low levels of current expression (Tang, C.-Y., C. T. Schulteis, R. M. Jiménez, and D. M. Papazian. 1998. *Biophys. J.* 75:1263–1270). Our findings demonstrate that heterologous expression of channels in *Xenopus* oocytes is a dynamic process influenced by cell physiology and development. These factors must be considered in interpreting the functional properties of heterologously expressed channels.

INTRODUCTION

K^+ channels play diverse and important roles in the modulation of membrane excitability and neuronal activity (Rudy, 1988; Hille, 1992; Rudy and Seeburg, 1999). Insights into the molecular structure of voltage-gated K^+ channel subunits have been obtained from studies on a number of K^+ channel genes first identified in *Drosophila*, including *Shaker* (Iverson et al., 1988; Pongs et al., 1988; Schwarz et al., 1988), *Shab, Shal, Shaw* (Wei et al., 1990; Covarrubias et al., 1991; Singh and Singh, 1999), and *eag* (Warmke et al., 1991; Ganetzky et al., 1999). These genes specify K^+ channel α-subunits with six transmembrane domains and a pore-forming region (Jan and Jan, 1997). Individual types of K^+ channel α-subunits can form functional homomultimeric channels (Iverson et al., 1988; Timpe et al., 1988), assembling as tetramers (MacKinnon, 1991; Li et al., 1992). In the *Xenopus* oocyte expression system, products of different splicing variants of the *Shaker* gene can form functional heteromultimeric K^+ channels (Isacoff et al., 1990; McCormack et al., 1990). Heteromultimeric K^+ channels have been demonstrated by in situ immunochemical studies in mammalian brains (Wang et al., 1993).

Genetic analysis in *Drosophila* has provided functional evidence for heteromultimeric assembly among different *Shaker* splicing variants (Haugland and Wu, 1990). Genetic evidence has also indicated interactions between Eag and Shaker (Sh) subunits (Wu and Ganetzky, 1992; Wu and Chen, 1995). *Shaker* mutations alter or eliminate the inactivating I_A current in adult and larval muscles (Salkoff and Wyman, 1981; Wu and Haugland, 1985), whereas *eag* mutations affect all four identified muscle K^+ currents including I_A (Wu et al., 1983; Zhong and Wu, 1991). Combined in double mutants, *eag* and *Shaker* produce synergistic phenotypes in an allele-dependent manner (Zhong and Wu, 1993). These results suggest that distinct K^+ channel subunit types such as Eag and Sh can functionally interact in vivo.

Mechanisms such as subunit coassembly into heteromultimeric channels (Wu and Ganetzky, 1986; 1992; Zhong and Wu, 1993; Wu and Chen, 1995) or the interplay among neighboring channels within protein clusters (Tejedor et al., 1997; Liu et al., 2000) allow the modulation of channel properties and enhance the diversity of K^+ channels to enrich the neurophysiological repertoires of neurons (Rudy and Seeburg, 1999). There is mounting evidence that heteromultimeric assembly can produce distinct functional properties in channel types that are also expressed as functioning homomultimers (e.g., Sh: Haugland and Wu, 1990; Isacoff et al., 1990; Wang et al., 1993; NMDA receptors: Monyer et al., 1992; Sheng et al., 1994; $GABA_A$ receptors: Barnard et al., 1998). It is also known that localization of ion channel clusters in subcellular regions is critical for the normal development and function of neurons. Well-established examples include the targeting of Ca^{2+} and K^+ channels and receptor-channels to pre and postsynaptic sites (Anderson and Cohen, 1977; Frank and Fischbach, 1979; Kim et al., 1995; Niethammer et al., 1996) and clustering of Na^+ channels in the nodes of Ranvier in myelinated nerve and electrocytes of electric fish (Aidley, 1998).

Received for publication 17 February 2000 and in final form 1 June 2000.
Address reprint requests to Dr. Chun-Fang Wu, Department of Biological Sciences, The University of Iowa, 138 Biology Building, Iowa City, Iowa 52242. Tel.: 319-335-1090; Fax: 319-335-1103; E-mail: cfwu@blue.weeg.uiowa.edu.

0006-3495/00/09/1358/11 $2.00

We have previously provided evidence for functional interactions between Sh and Eag channel subunits expressed in *Xenopus* oocytes (Chen et al., 1996). Coexpression of Sh and Eag polypeptides accelerates the decay time course and slows recovery from inactivation of the transient Sh-like current, measured 3 to 6 days after RNA injection. A subsequent study reported an absence of such interactions (Tang et al., 1998). In that report, currents of small amplitudes were recorded 1–2 days after injection with lower amounts of RNA. Taken together, these two studies suggested that channel expression level and coexpression time course may influence functional interactions between Sh and Eag channel subunits in oocytes.

Our aim in this study was to elucidate the cellular conditions that promote functional interactions between Sh and Eag subunits in the *Xenopus* oocyte system. The results obtained not only confirm our earlier description of a functional interaction between Eag and Sh subunits (Chen et al., 1996), but also replicate the observation of Tang et al. (1998) at low expression levels. Our study establishes that expression levels and developmental time are important factors for channel subunit interactions and therefore must be considered for the proper interpretation of heterologous expression experiments in the *Xenopus* oocyte system.

METHODS

Channel expression

The Eag cDNA was kindly provided by G. Robertson, University of Wisconsin, Madison, WI (Chen et al., 1996). The ShB and Eag RNAs were prepared using a commercial RNA transcription kit that uses the T7 RNA promoter (Ambion, Austin, TX). The yield of RNAs was estimated to be ~10 μg per reaction by using the standard RNA ladder. The RNA products were then dissolved in 40 μl RNAase-free water, aliquoted, and stored at −20°C. The ShBT449V and ShB-CEag constructs were prepared as described previously (Chen et al., 1996).

Oocytes were isolated and prepared for RNA injection as described (Chen et al., 1996). The isolated oocytes were kept at 16°C and RNA injection was carried out 1 day after isolation. The relative functional expression levels of the Eag and ShB subunits were manipulated by injecting different amounts of the corresponding RNAs to give similar peak current amplitudes in singly injected oocytes. This was achieved by diluting the RNA stock solutions to different final concentrations and injecting 40 nl of solution into each oocyte. The estimated quantities of the RNAs injected varied from 2 to 8 ng/oocyte for ShB and 0.05–0.2 ng/oocyte for Eag, as specified in the figure legends. The amounts of the two messages injected were adjusted such that the Eag and Sh currents had a comparable amplitude 3 to 6 days after injection. For coexpression of Eag and ShB, 40 nl of solution was injected containing the same quantities of the respective RNAs used for singly injected oocytes. Because different batches of oocytes expressed at different efficiencies, in each experiment the same batch of oocytes was used for injection of all different messages to facilitate comparisons.

Electrophysiology

Whole-oocyte currents were recorded with a two-electrode voltage clamp amplifier (model OC-725 B, Warner, Hamden, CT). The electrodes, filled with 3 M KCl, had a typical initial resistance of 0.1–0.5 MΩ. The bath solution contained (in mM): 140 NaCl, 2 KCl, 2 $MgCl_2$, and 10 HEPES, pH 7.2. In some experiments noted in the figure legends, the concentration of $MgCl_2$ was increased to 10 mM to facilitate kinetic separation of the Eag and ShB currents. The bath ground electrodes were placed immediately adjacent to the cell (within 2 mm) to minimize errors attributable to the bath series resistance. All experiments were performed at room temperature (20–22°C).

Macropatch recordings were made in a solution containing (in mM): 140 KCl, 2 $MgCl_2$, 11 EGTA, and 10 HEPES (*N*-methylglucamine [NMG], pH 7.2), using an Axopatch 200A amplifier (Axon Instruments, Foster City, CA). Borosilicate glass pipettes coated with dental wax had a typical initial resistance of 0.2–0.6 MΩ.

Data acquisition and analysis were performed with Apple Macintosh computers using Pulse/Pulse Fit (HEKA, Lambrecht, Germany) and Igor (Wavemetrics, Lake Oswego, OR) software. Leak and capacitive currents were corrected using a modified P/n protocol. To examine whether the Eag and ShB subunits do interact, the weighted Eag and ShB components were summed to simultaneously fit the peak and the steady-state levels of the coexpressed current. In addition, the weighted Eag current was subtracted from the Eag-ShB coexpressed current and the resulting waveform was compared with the ShB current (cf. Fig. 1 *B* in Chen et al., 1996).

RESULTS

Eag and ShB interaction depends on subunit expression levels

In these experiments, as in previous studies (Chen et al., 1996; Jan and Jan, 1997; Ganetzky et al., 1999), injection of Sh RNA induced a transient K^+ current, whereas injection of Eag RNA induced a noninactivating K^+ current. We previously showed that coexpression of Sh and Eag accelerated the inactivation kinetics of the transient Sh current (Chen et al., 1996). The expression efficiency of Eag was greater than that of ShB with equivalent RNA injection, as indicated by the amounts of each RNA required to produce equivalent current amplitudes in singly injected oocytes (see Methods; Fig. 1). Such a difference could arise at several levels, including RNA stability, translation, post-translational modification, and localization of the protein products. Because of this difference in functional expression, the interaction between Eag and ShB subunits was better observed with a lower dose of Eag RNA relative to ShB RNA (Chen et al., 1996).

If the Eag and ShB subunits only form functionally independent channels, it should be possible to use a linear summation of Eag and ShB components to fit the coexpressed waveforms (cf. Covarrubias et al., 1991; Chen et al., 1996). Tang et al. (1998) reported that coexpression of Sh and Eag subunits produced a current identical to the sum of the currents in singly injected oocytes, indicating no interaction between the Sh and Eag proteins. The quantities of RNA injected in their study were 0.1–0.5 ng/cell for ShB and an equivalent or greater amount for Eag (Tang et al., 1998), in contrast to 8–10 ng ShB and 0.1–0.5 ng Eag RNA/cell in our previous study (Chen et al., 1996). It is possible that the density of channel subunits expressed in oocytes could affect the degree of interactions among different types of K^+ channel subunits.

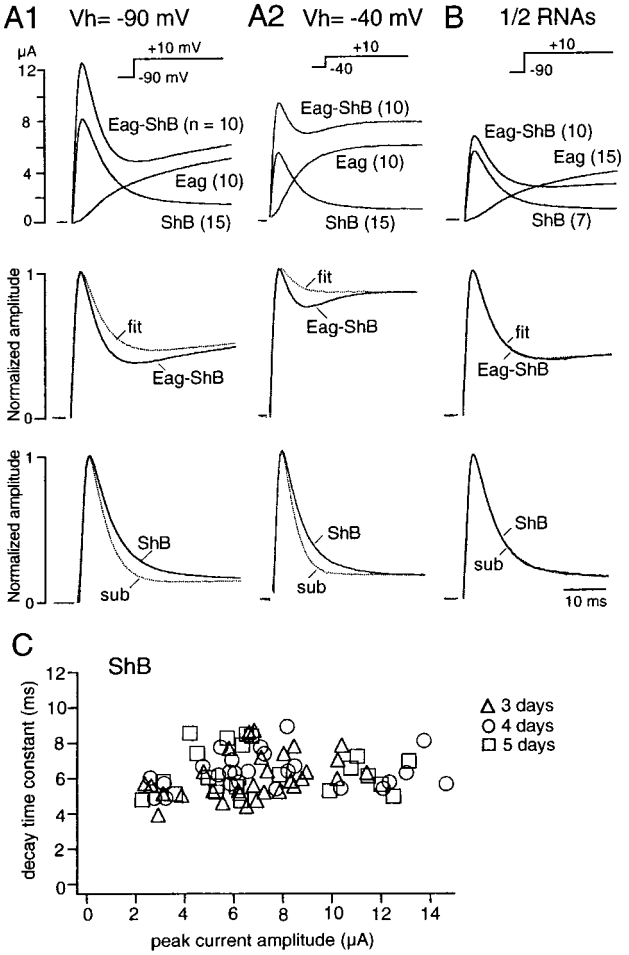

FIGURE 1 Lower current expression reduces Eag-Sh interaction. (*A1*, *top*) Averaged waveforms obtained 5 days after injection of Eag RNA (0.1 ng/cell), ShB RNA(4 ng/cell), or 0.1 ng Eag plus 4 ng ShB RNA, in response to a step from −90 mV to +10 mV. Numbers of oocytes are given in parentheses. *Middle and bottom:* The coinjection waveform cannot be fit by a linear summation of single currents. The coexpressed Eag-ShB waveform is superimposed with the weighted waveform (*fit*) which was obtained by a linear summation of Eag and ShB components, weighted to achieve the best fit for both the peak and steady-state current amplitudes (fit = 1.52 ShB + 0.85 Eag). The normalized ShB waveforms are compared with the subtracted (*sub*) waveforms in which the weighted Eag component has been subtracted from the Eag-ShB (sub = Eag-ShB − 0.85 Eag). (*A2*) The same set of oocytes presented in *A1* but held at −40 mV and stepped to +10 mV. Even with smaller peak current amplitudes, the Eag-ShB waveform cannot be fit by a linear summation (fit = 1.55 ShB + 1.10 Eag, and sub = Eag-ShB − 1.10 Eag). (*B*) Averaged waveforms recorded from oocytes injected with Eag RNA (0.05 ng/cell), ShB RNA (2 ng/cell), or 0.05 ng Eag plus 2 ng ShB RNA, in response to a step from −90 mV to +10 mV. There is no interaction observed as late as 5 days after injection. The averaged Eag-ShB-induced waveform could be fit by a linear summation (fit = 1.20 ShB + 0.49 Eag). (*C*) Scatter plot shows the relationship between the decay time constant and the peak current amplitude of ShB currents measured 3 (*triangles*), 4 (*circles*), and 5 days (*squares*) after ShB RNA injection. Five-day data are the same as shown in panels *A* and *B*. All data were collected from the same batch of oocytes.

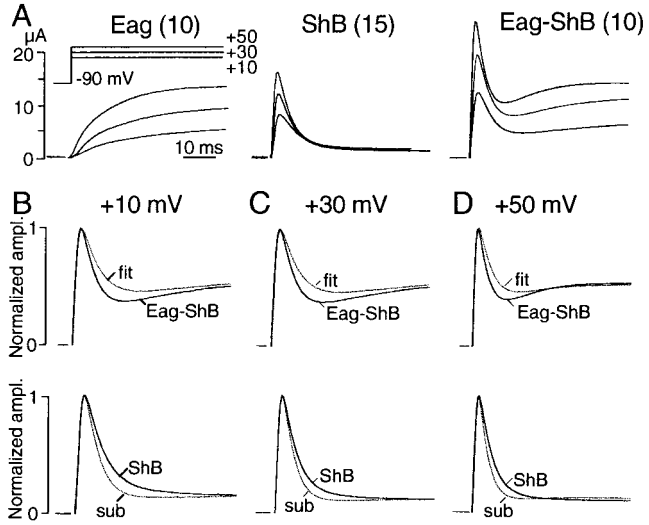

FIGURE 2 Interaction between Eag and Sh subunits observed at different voltages. (*A*) Averaged traces recorded from same oocytes as Fig. 1 *A1* (numbers of oocytes in parentheses), 5 days after RNA injection, in response to steps from −90 mV to +10, +30 and +50 mV. (*B*) Voltage stepped to +10 mV. Fit = 0.85 Eag + 1.515 ShB and sub = Eag-ShB − 0.85 Eag. (*C*) Voltage stepped to +30 mV. Fit = 1.57 ShB + 0.96 Eag and sub = Eag-ShB − 0.96 Eag. (*D*) Voltage stepped to +50 mV. Fit = 1.55 ShB + 0.82 Eag and sub = Eag-ShB − 0.82 Eag.

To examine this possibility, we adjusted the amounts of Eag and ShB RNAs injected per cell. As shown in Fig. 1 *A1*, 5 days after injection with Eag RNA (0.1 ng/cell), ShB RNA (4 ng/cell), or both, the coexpressed waveform (in response to pulses from −90 to +10 mV) could not be fit by a linear summation of the Eag and ShB waveforms. In Fig. 1 *A1* (*bottom panel*) the normalized ShB waveform is compared with the subtracted waveform in which the weighted Eag component has been subtracted from the coexpressed Eag-ShB waveform. The acceleration of inactivation of the transient currents in the coinjected oocytes is evident in these comparisons.

A very different result was observed when the amount of RNA injected was reduced. Fig. 1 *B* (*top panel*) shows the averaged traces recorded from oocytes injected with reduced Eag RNA (0.05 ng/oocyte), ShB RNA (2 ng/oocyte), or both Eag and ShB. The averaged Eag-ShB waveform recorded from these lower expression oocytes could be fit by a linear summation of the Eag and ShB currents that were separately expressed (Fig. 1 *B*, *middle panel*). Moreover, the normalized ShB waveform is identical to the subtracted waveform (Fig. 1 *B*, *bottom panel*).

Tang et al. (1998) raised the possibility that series resistance errors, expected to be more pronounced at greater current amplitudes, could have contributed to the observed acceleration in the decay time course of the coexpressed currents in our earlier study (Chen et al., 1996). In their report, only oocytes that expressed currents with amplitudes

between 1 and 15 μA were analyzed. In the present study the following observations argue against the possibility of an artifact introduced by series resistance errors. The same batch of oocytes shown in Fig. 1 *A1* was held at a less negative potential (−40 instead of −90 mV) to partially inactivate the transient Sh current (Fig. 1 *A2*). Under these conditions, the transient ShB currents were reduced to an amplitude similar to those seen with low doses of RNA injection and holding potentials of −90 mV (compare Fig. 1 *A2* and 1 *B*). However, these small-amplitude currents still could not be fit by a linear summation (Fig. 1 *A2*). Furthermore, the scatter plot (Fig. 1 *C*) using the same oocytes shown in Fig. 1, *A* and *B* shows no dependence of the decay time constant on the peak amplitude of the ShB currents expressed in oocytes 3–5 days after RNA injection (see Fig. 3 *C* for another analysis including a wider range of current amplitudes).

To minimize any series resistance errors and to ensure good voltage clamping control, most results shown in this report correspond to currents activated by depolarizing steps to +10 mV. However, data collected with more depolarized voltages (+30 and +50 mV) yielded results consistent with those of +10 mV. Fig. 2 compares results for steps to +10, +30, and +50 mV, obtained from the same oocytes shown in Fig. 1 *A*.

Developmental progression of K^+ current expression after RNA injection

Our previous study (Chen et al., 1996) showed functional interactions between coexpressed Eag and Sh subunits 3–6 days after RNA injection. Tang et al. (1998) reported an absence of interaction between coexpressed Eag and Sh subunits based on data collected between 1 and 2 days after RNA injection. This discrepancy suggested that sufficient developmental time may be required for such interactions to appear.

To address this, we first examined the progression of K^+ current expression. Each oocyte was injected with 0.2 ng Eag RNA, 8 ng ShB RNA, or 0.2 ng Eag RNA plus 8 ng ShB RNA. The Eag- and ShB-induced currents observed on different days after RNA injection are compared to the currents induced by coinjection in Fig. 3 *A*. All data shown were obtained from the same batch of oocytes because of variation in functional expression efficiency between batches (see Methods). There were obvious increases in the amplitudes of expressed currents over time within the 6-day observation period. The Eag current amplitude developed more slowly than ShB in the early days of observation, but was still increasing after the ShB current had plateaued on days 5–6. Interestingly, we found that both Eag and ShB

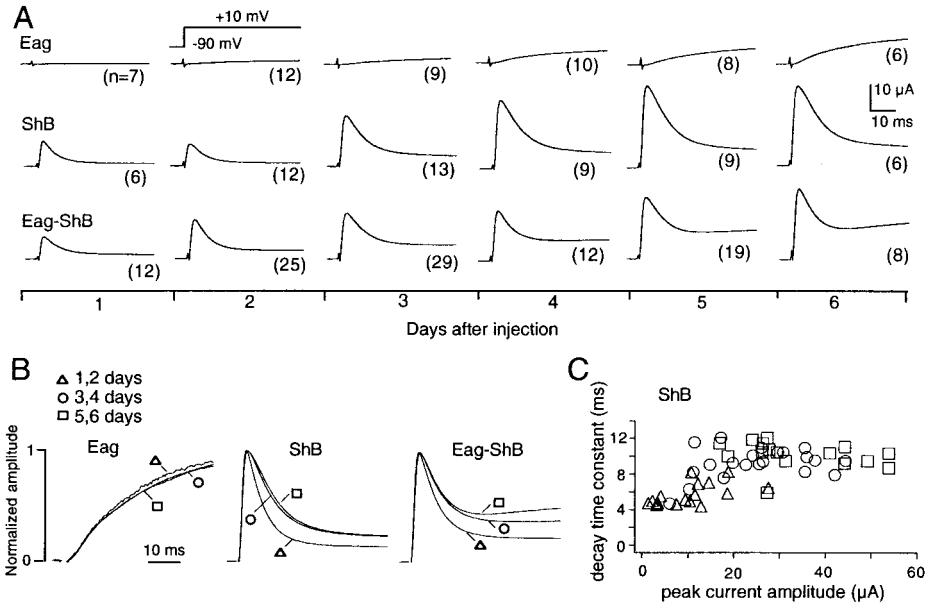

FIGURE 3 Developmental progression of K^+ currents heterologously expressed in *Xenopus* oocytes. (*A*) K^+ currents recorded from oocytes after different periods after injection with Eag RNA (0.2 ng/oocyte), ShB RNA (8 ng/oocyte), or Eag and ShB RNAs together (0.2 ng Eag + 8 ng ShB RNA/oocyte), in response to a step from −90 to +10 mV. All data were collected from a single batch of oocytes. Each trace represents the mean of responses from the number of oocytes indicated in parentheses. (*B*) Averaged waveforms of Eag- and ShB-induced currents and the coexpressed current (Eag-ShB) were normalized to peak amplitude and superimposed. Age dependence of kinetic change is apparent in ShB and Eag-ShB, but not Eag. (*C*) The scatter plot shows the relation between the decay time constant and the peak current amplitude of ShB current on different days after ShB RNA injection: 1–2 days (*triangles*), 3–4 days (*circles*), and 5–6 days (*squares*). Note that most low-amplitude data points correspond to young (1–2-day) oocytes, which have faster decay kinetics. Among 3–6-day oocytes, decay time constants do not appear correlated with current amplitude.

RNAs expressed even larger currents when they were injected into oocytes that had been isolated for 4 days (data not shown), rather than 1 day, as in our standard protocol.

To determine whether kinetic changes also occurred over time, we normalized and superimposed the averaged traces collected at early (after 1–2 days), middle (3–4 days), and late (5–6 days) developmental stages (Fig. 3 *B*). It can be seen that the kinetics of Eag currents recorded on different days are identical despite great differences in their amplitudes (*left panel*). In contrast, the decay kinetics of ShB currents became slower between 1–2- and 3–4-day stages and reached a plateau thereafter (*middle panel*), and the same was true for the Eag-ShB coexpressed currents (*right panel*). The decay time constants of ShB currents collected from different days after RNA injection are presented in Fig. 3 *C*. It can be seen that the decay time constants of ShB currents were shorter on the first and second days (cf. Fig. 3 *B*). Data collected from the middle and late developmental stages indicated no dependence of the decay time constant on the peak current amplitude (Fig. 3 *C*), despite a wider range of amplitudes than in Fig. 1 *C*.

Acceleration of inactivation kinetics of the transient current in coinjected oocytes depends on developmental time

We next examined whether the interaction between Eag and ShB currents changed over time. The data from Fig. 3 *A* were pooled into groups of 1–2, 3–4, and 5–6 days after RNA injection (Fig. 4, *top panels*). Beyond 1–2 days after injection, the coexpressed Eag-ShB waveform showed slightly slower decay than the fitted waveform (Fig. 4 *A*, *middle panel*). The ShB waveform also differed only slightly from the subtracted waveform (Fig. 4 *A*, *bottom panel*). On 3–4 days after injection, the inactivation kinetics of the transient current in Eag-ShB became slightly faster than the weighted waveform (Fig. 4 *B*). The acceleration of inactivation kinetics of the transient currents became pronounced 5–6 days after injection (Fig. 4 *C*). The age-dependent acceleration of inactivation kinetics was consistently observed in different batches of oocytes with the same amount of RNAs injected (data not shown).

It might be asked whether the observed increase in Eag-ShB interactions is a secondary effect of increased levels of current expression over time. We analyzed those oocytes at an early developmental stage (selected from 1-day oocytes shown in Fig. 3) that had high levels of current expression (>20 μA peak current for both ShB, $n = 3$, and Eag-ShB, $n = 6$). Even with high levels of expression, the coexpressed current could be fit by weighted Eag and ShB components (data not shown). Conversely, we analyzed aged oocytes (selected from 5-day oocytes shown in Fig. 1 *A1*) that expressed lower amplitudes of currents (<20 μA for both ShB, $n = 9$, and Eag-ShB, $n = 2$). In this case, the coexpressed current still could not be fit by weighted Eag and ShB components (data not shown). These observations indicate that developmental time is important for functional interactions among coexpressed Eag and Sh subunits.

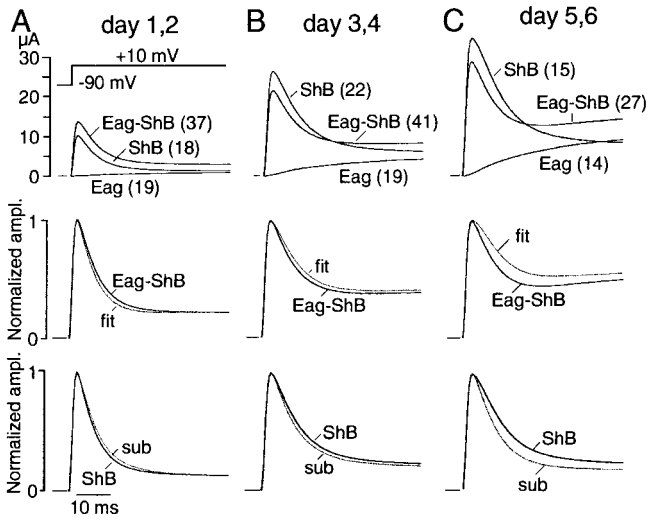

FIGURE 4 Acceleration of inactivation of the transient currents induced by coinjection increases with age. Same data as Fig. 3, combining subsets (*A*) 1–2 days, (*B*) 3–4 days, and (*C*) 5–6 days. In the middle panels the coexpressed Eag-ShB waveform is superimposed with the linear sum of Eag and ShB components (*fit*). For 1–2 days: fit = 1.35 ShB + 1.20 Eag; 3–4 days: 0.82 ShB + 0.88 Eag; 5–6 days: 0.82 ShB + 1.00 Eag. In the bottom panels the normalized ShB waveforms are compared with the subtracted (*sub*) waveforms. For 1–2 days: sub = Eag-ShB − 1.20 Eag; 3–4 days: Eag-ShB − 0.88 Eag; 5–6 days: Eag-ShB − 1.00 Eag.

High Mg^{2+} slows the activation kinetics of Eag current and more clearly reveals the interaction between Eag and ShB subunits

Increasing the Mg^{2+} concentration in saline can slow the activation kinetics of the Eag current (Terlau et al., 1996). Fig. 5 *A1* shows the averaged traces recorded from oocytes 3 days after injection with RNAs of Eag (0.2 ng/cell), ShB (8 ng/cell), and Eag plus ShB (0.2 ng Eag + 8 ng ShB RNA/cell), in response to steps from −90 to +50 mV. Each set of data presents averaged traces obtained from the same oocytes, first bathed in 2 mM Mg^{2+} and then in 10 mM Mg^{2+} saline. High Mg^{2+} only affects the Eag activation kinetics and does not noticeably change the ShB waveform (Fig. 5 *A1*). Fig. 5 *A2* shows that in 10 mM Mg^{2+} saline, the discrepancy between the Eag-ShB waveform and the fitted waveform was much more noticeable.

With high Mg^{2+} the progression of interactions over developmental time was even more evident. Fig. 5 *B1* shows averaged currents recorded from aged oocytes (6 days) that expressed transient current amplitudes similar to those of the 3-day oocytes shown in Fig. 5 *A1*. The enhancement of the discrepancy between the coexpressed and fitted currents in the presence of high Mg^{2+} was more pro-

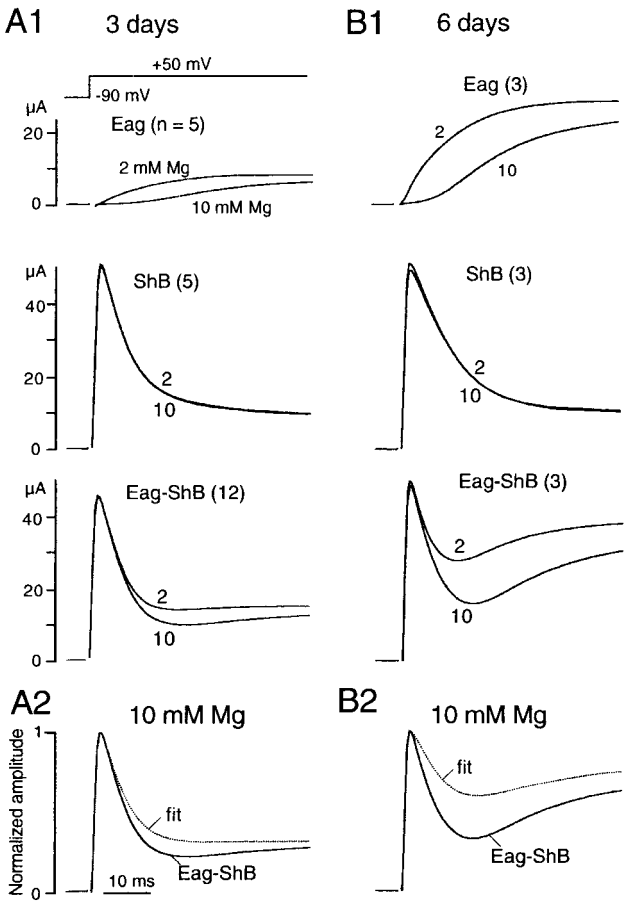

FIGURE 5 High Mg^{2+} in saline slows the activation kinetics of the *eag* current and more clearly reveals Eag-ShB interactions. (*A1*) 3 days after injection with Eag RNA (0.2 ng/oocyte), ShB RNA (8 ng/oocyte), or 0.2 ng Eag RNA plus 8 ng ShB RNA/oocyte, currents were recorded in either 2 mM or 10 mM Mg^{2+} saline. The voltage pulse was stepped from −90 to +50 mV. (*A2*) In 10 mM Mg^{2+} saline, fit = 0.96 ShB + 0.89 Eag. (*B1*) Currents recorded 6 days after injection. (*B2*) In 10 mM Mg^{2+} saline, fit = 0.98 ShB + 1.15 Eag.

nounced in these aged oocytes than in 3-day oocytes (compare Fig. 5, *A2* and *B2*). Furthermore, the discrepancy was much greater than that observed in 2 Mg^{2+} saline (compare Fig. 5 *B2* and Fig. 4 *C*).

A different approach can be used to enhance the kinetic separation between the transient and delayed currents in normal saline. A delay of Eag current activation can be achieved by strong hyperpolarization (Hille, 1992). A hyperpolarization prepulse protocol (−130 or −150 mV) led to a similar enhancement of the acceleration of transient component decay kinetics in coinjected oocytes (data not shown).

Simultaneous RNA injection promotes Eag and ShB subunit interaction

We previously showed that preformation of ShB channels followed by Eag RNA injection results in separate Eag and ShB currents with no indication of Eag-ShB interaction (Chen et al., 1996). To confirm that simultaneous expression of the two subunit types promotes their interaction, we examined whether preformed Eag subunits could interact with subsequently expressed Sh subunits. Fig. 6 *A* shows averaged traces in response to a pulse from −90 to +50 mV, measured 5 days after injection of Eag RNA (0.2 ng/oocyte), ShB RNA (8 ng/oocyte), or both Eag and ShB. Other oocytes received sequential injection of Eag RNA (0.2 ng/cell) and then ShB RNA (8 ng/oocyte) 3 days later, and experiments were performed 5 days after the first injection (Fig. 6 *B*). (Systematic comparisons after longer developmental times were not possible because many oocytes degraded after 7 days.) A linear summation of the ShB and Eag waveforms can fit the currents from the sequential injection oocytes (Fig. 6 *B*, *bottom panel*). The same is true when the injection sequence was reversed (Fig. 6 *C*), consistent with our previous observations (Chen et al., 1996).

Coinjection of ShB with ShB-CEag slows recovery from inactivation

The C-terminus of Eag is the region most distinct from other families of K^+ channel subunits (Warmke et al., 1991), and it has been reported that the C-terminal domain mediates assembly of the voltage-gated rat EAG potassium channel (Ludwig et al., 1997). Therefore, this domain may play a role in the interaction between Eag and Sh subunits. We previously constructed a chimeric ShB subunit, ShB-CEag, in which the ShB cytoplasmic carboxyl domain was replaced with the Eag carboxyl terminus (Chen et al., 1996). This construct does not express noticeable currents when expressed alone, but markedly accelerates the decay of transient currents when coexpressed with ShB, as previously shown at high peak current amplitudes (20.3–49.7 μA, Chen et al., 1996).

Here we took advantage of the reduced interference of noninactivating currents with transient current measurements in oocytes coinjected with ShB and ShB-CEag RNA to firmly establish subunit interactions at a reduced current level activated at a lower voltage (stepping from −90 to −10 mV for 4.6–12.8 μA peak amplitudes, Fig. 7 *A*). Coexpression of ShB with ShB-CEag reduced the amplitudes of both the transient and steady-state components compared to those induced by ShB expression alone (Fig. 7 *A*), even though the same amount of ShB RNA was injected in both cases. A discrepancy between the coexpressed and fitted currents was clear in both the decay kinetics and the steady-state component (see normalized traces in Fig. 7 *A*, *bottom panel*). Because of the low current amplitudes, the accelerated decay of the coexpressed current is not likely to be due to clamping error.

We previously showed that coexpression of ShB and Eag slowed the recovery from N-type inactivation of the transient component (Chen et al., 1996; cf. Hoshi et al., 1991),

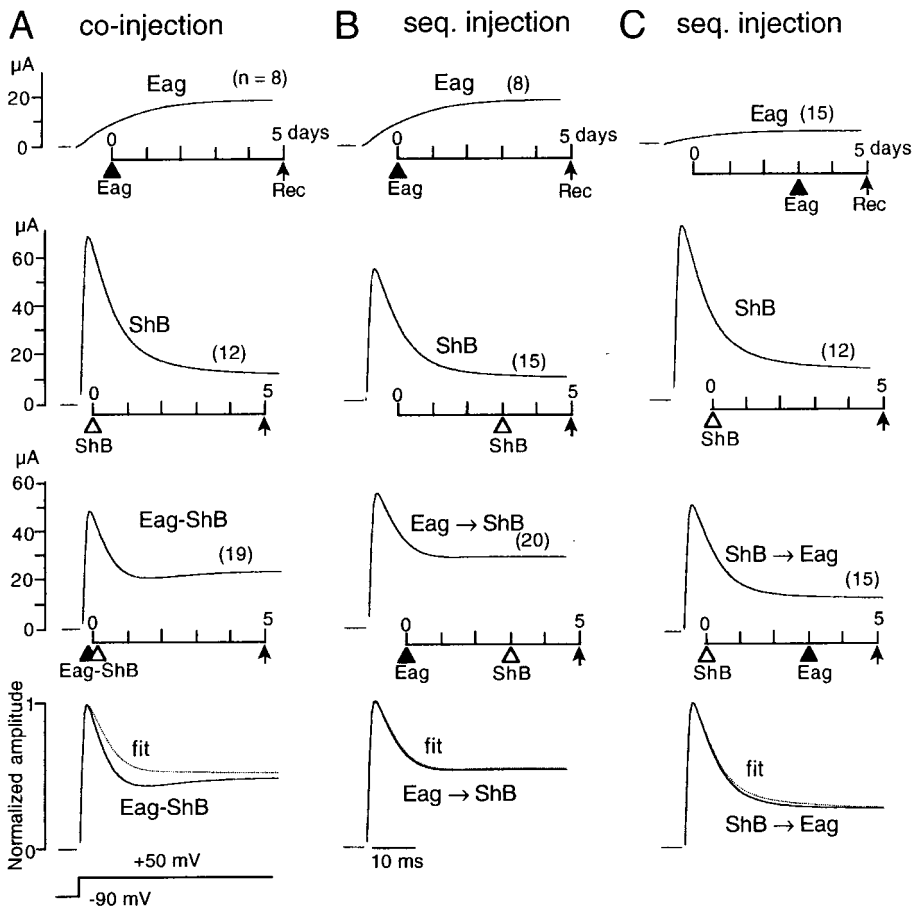

FIGURE 6 Simultaneous injection of Eag and ShB RNAs promotes the interaction between subunits. All data were collected from a single batch of oocytes. (*A*) Averaged traces from injections of Eag (0.2 ng/oocyte) and ShB RNA (8 ng/oocyte) alone and from coinjection of their RNAs (0.2 ng Eag RNA plus 8 ng ShB RNA/oocyte). The voltage pulse was stepped from −90 to +50 mV. The averaged Eag-ShB waveform could not be fit by linear summation. Fit = 0.69 ShB + 0.88 Eag. (*B*) Sequential injection of Eag and ShB RNAs. Eag RNA (0.2 ng/oocyte) was injected first and ShB RNA (8 ng/oocyte) 3 days later. Recordings were performed 5 days after the initial injection. The averaged Eag-ShB waveform (Eag → *ShB*) could be fit by a linear summation (Fit = 1.00 ShB + 1.07 Eag). (*C*) Sequential injection of ShB and Eag RNAs. ShB RNA was injected first and Eag RNA 3 days later. Recordings were performed 5 days after the initial injection. The averaged ShB-Eag waveform (*ShB* → *Eag*) could be fit by a linear summation (fit = 0.75 ShB + 0.92 Eag).

which could indicate changes in the affinity between the N-terminus of Sh and the acceptor domain. We asked whether the Eag C-terminus is sufficient to affect recovery from inactivation when coexpressed with ShB. Examples of the recovery from inactivation of the ShB and coexpressed currents are shown in Fig. 7 *B*. We selected oocytes with similar amplitudes of ShB and coexpressed currents to reduce the possibility of clamp error. It is clear that coexpression of ShB with ShB-CEag slowed the recovery from inactivation when the interpulse intervals were shorter than 160 ms (Fig. 7, *B* and *C*). This is presumably due to interference with recovery from N-type inactivation because the slow component of recovery from C-type inactivation was apparently not affected (Fig. 7 *C*, beyond 160 ms, cf. Hoshi et al., 1991).

Interaction between Eag and ShBT449V subunits is reduced upon macropatch excision

In our previous report (Chen et al., 1996) we used the ShBT449V channel, which retains N-type inactivation but lacks C-type inactivation, to demonstrate that coexpression with Eag specifically alters N-type inactivation. Here we used the macropatch technique to increase voltage clamp fidelity and to investigate the influence of cytoplasmic conditions. Fig. 8 (*top panels*) shows superimposed current traces from sequential recordings in cell-attached and excised inside-out configurations, from an oocyte injected with the ShBT449V RNA alone and one with both ShBT449V and Eag RNAs. The time constant of the current decay and the near-steady-state current amplitude (30 ms after the depolarization onset, when the Eag component is becoming fully activated) are also shown (Fig. 8, *bottom panels*).

In the cell-attached configuration, the decay time constant was faster in the coexpressed current than in ShBT449V, confirming the earlier results of Chen et al. (1996). In the coinjected cell, a noticeable proportion of the current at 30 ms reflects the delayed activation of the Eag component, which was absent in the ShBT449V-injected cell (Fig. 8). Upon patch excision, the decay time constant of the ShBT449V current accelerated slightly, but abruptly. In contrast, the decay time constant of the coexpressed current gradually increased to a level similar to the time constant of ShBT449V. Concomitant with the gradual slowing of the current decay, the Eag current amplitude at 30 ms after the pulse onset progressively declined to a new stable value, indicating the rundown of the Eag component. These

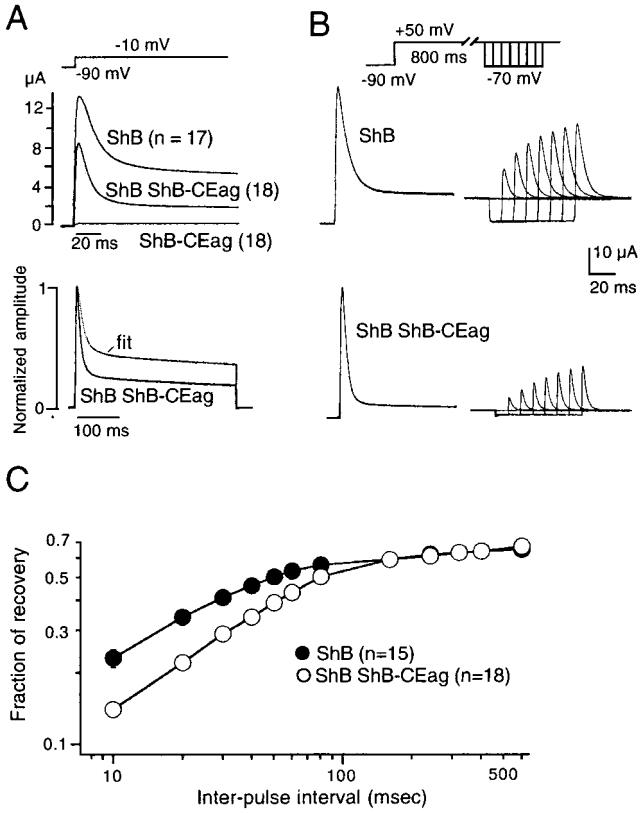

FIGURE 7 Eag C-terminus plays a role in acceleration of inactivation and retardation of recovery. (*A*) Averaged currents recorded after injection of ShB-CEag RNA (5 ng/oocyte), ShB RNA (5 ng/oocyte), or both messages (5 ng ShB plus 5 ng ShB-CEag RNA/oocyte), in response to pulses from −90 stepped to −10 mV. There was little expression of ShB-CEag-induced current and the ShB ShB-CEag coexpressed waveform could not be fit by linear summation (fit = 0.63 ShB). (*B*) Examples of twin-pulse responses of ShB and ShB ShB-CEag coexpressed currents. Two 800-ms pulses from −90 to +50 mV, separated by different interpulse intervals between 10 and 70 ms, were given at 12-s intervals. (*C*) The relation between the interpulse intervals (10–600 ms) and the fractional recovery from inactivation. Data were collected from a single batch of oocytes 3–5 days after RNA injection. Open circles represent the coinjected oocytes and filled circles represent the ShB-expressed currents. Each point presents the mean ± SE from the number of oocytes indicated. Error bars are smaller than symbols.

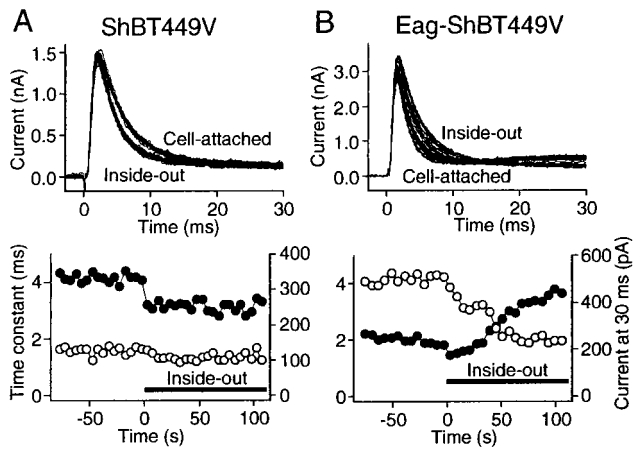

FIGURE 8 Macroscopic currents were recorded from oocytes expressing ShBT449V alone (*A*) and coexpressing Eag and ShBT449V (*B*) using the macropatch method. Pulses from −90 to 0 mV were applied at 5-s intervals. At $t = 0$, the patch was excised to change from the cell-attached configuration to the inside-out configuration. Current amplitudes at 30 ms after pulse onset (*open circles*) and time constant values (*filled circles*) are plotted as a function of time in the experiment. Note that in the Eag-ShBT449V group, patch excision decreased the Eag component (i.e., rundown) and also increased the apparent inactivation time constant.

results show that patch excision causes both a loss of the accelerated decay of the transient current and rundown of the Eag component in the coinjected oocyte. Thus, cytoplasmic factors, such as cytoskeletal elements, are likely to be involved in acceleration of the transient current by Eag coexpression.

DISCUSSION

We have demonstrated that the properties of Eag and ShB channels, heterologously expressed or coexpressed in *Xenopus* oocytes, are critically influenced by the level and time of expression. Under appropriate expression conditions, coexpressed currents cannot be fit by a linear summation of singly expressed Eag and Sh currents. Inactivation of the transient Sh-type current is accelerated in coinjected oocytes (Figs. 1, 2, 4–7) (Chen et al., 1996), indicating interactions between Eag and Sh polypeptides. We compared the extent of interaction using different amounts of RNA injection, and traced the development of currents over time after RNA injection. The acceleration of decay was not observed with low amounts of RNA injection (Figs. 1 and 2), or earlier than 3 days after injection (Figs. 3 and 4). Resolution of the interaction was increased further by comparing results within a single batch of oocytes to reduce variation, and by confirming results with protocols producing small currents to minimize clamping error due to series resistance. Interactions were even more noticeable under conditions that slowed the activation kinetics of Eag and rendered the delayed current component more easily separated from the fast-activating early transient. These included using 10 mM Mg^{2+} saline (Fig. 5) and a hyperpolarizing prepulse protocol (data not shown; see Results). Sequential RNA injection experiments (Fig. 6) and macropatch recordings (Fig. 8) revealed further information about conditions for the subunit interaction. Newly expressed subunits were prevented from interacting with preformed functional channels (Fig. 6). Upon macropatch excision, rundown of the Eag current component abolished the acceleration of the Sh current decay (Fig. 8). In addition to accelerated decay, interference with recovery from N-type inactivation in coexpressed currents is a further indication that Eag and ShB subunits interact (Chen et al., 1996). Here

we show that coexpression of ShB with ShB-CEag reproduced these two properties, establishing a role for the Eag C-terminus in modifying the recovery from, as well as the onset of, N-type inactivation (Fig. 7). These observations bring together and replicate the differing results of two previous studies (Chen et al., 1996; Tang et al., 1998) while providing new information about conditions that promote functional interactions between two well-studied K^+ channel subunits in the *Xenopus* oocyte heterologous expression system.

Functional significance

K^+ channels play essential roles in neural function, and mutations of K^+ channels are responsible for human diseases (e.g., Sanguinetti et al., 1995; Zerr et al., 1998) and mammalian neuropathologies (e.g., Silverman et al., 1996; Pardo et al., 1999). It will be of interest to determine whether these channel subunits interact with other channel types in vivo, because of the important implications for nervous system functioning. Our results provide support for the idea that Eag and ShB channel polypeptides interact in vivo, either through physical/chemical coupling or by coassembly into heteromultimeric channels. Examples of both mechanisms of interaction are known. There are precedents for heteromultimeric associations of channel subunits that can also express functioning channels when expressed singly in oocytes. These include Sh channels (Isacoff et al., 1990; Wang et al., 1993) and NMDA (Monyer et al., 1992; Sheng et al., 1994) and $GABA_A$ (Barnard et al., 1998) receptor channels. If the interaction of Eag and ShB shown here were mediated by coassembly of the subunits, this would be the first case of heteromultimeric assembly of different K^+ families (cf. Covarrubias et al., 1991). This would set the stage for a combinatorial mechanism that would greatly increase the variety of channel properties that could be achieved (Wu and Chen, 1995).

Interaction of different channels in local clusters is also known. For example, direct protein-protein contact allows functional cross-talk between dopamine and $GABA_A$ receptors (Liu et al., 2000). Furthermore, multiple members of the PSD-95 family of membrane-associated guanylate kinases play important roles in receptor and channel clustering that could be critical for signal transduction within and between neurons (Kim et al., 1995; Niethammer et al., 1996). It has been shown that the clustering of Sh and glutamate receptor channels in *Drosophila* neuromuscular junctions are disrupted by mutations of *dlg*, a gene encoding a member of the PSD-95 family (Tejedor et al., 1997). In preliminary experiments we injected a mixture of RNAs (0.2 ng Eag, 5 ng ShB, and 2.5 ng PSD-95/cell) and found that PSD-95 abolished the interactions between Eag and ShB in oocytes (M. L. Chen, T. Hoshi, C.-F. Wu, unpublished data). This is consistent with the notion of interactions between homomultimeric Eag and Sh channels in close contact within clusters. The loss of the interaction upon macropatch excision suggests that the acceleration of N-type inactivation in macropatch experiments also depends on cytoplasmic factors.

The present results showing interactions between Eag and ShB channel subunits in a heterologous expression system are consistent with genetic studies in *Drosophila*. The four K^+ currents in larval muscle, with different kinetics and properties, are all modified in *eag* mutants, yet no current is entirely eliminated by *eag*, suggesting a contribution of the Eag subunit to several different channel types (Zhong and Wu, 1991). In addition, mutations of *eag* and *Sh* genes show allele-dependent interactions in muscle (Zhong and Wu, 1993). The exact *Sh* splicing variants expressed in muscle have not been identified, and cellular conditions may differ between native cells and *Xenopus* oocytes. Nevertheless, in vivo findings imply that Eag and Sh products interact either within heteromultimeric channels or between neighboring channels.

Factors important to subunit interactions

Little systematic attention has been given to the effects of expression level and time on interpreting data from oocyte expression experiments. However, indications of the importance of expression level have been reported. For example, it has been shown for ShH4 messages (Moran et al., 1992) and brain Kv1.2 (Guillemare et al., 1992) that the level of expression controls modes of gating and modifies pharmacological sensitivities of K^+ channels expressed in oocytes. In addition, interactions occurring at a high density of heterologously expressed glycine receptors modify the agonist response and may contribute to neurotransmitter efficacy at fast synapses (Taleb and Betz, 1994). Finally, a human K^+ channel (HLK3) displays different inactivation kinetics induced by high-concentration RNA injection, possibly due to channel clustering involving cytoskeletal elements (Honoré et al., 1992). Our findings are consistent with the above studies in showing that physiological expression levels can change the functional properties of Eag and ShB channel subunits. We have further demonstrated the importance of developmental time of expression in the oocyte system as a primary factor for the interaction to appear, not simply a secondary effect of increased expression levels over time.

It is interesting to note a correlation between the quantities of RNA injected and the difference in amplitudes between the transient current in coinjected oocytes and the peak current in ShB-injected oocytes. With 0.05 ng Eag and 2 ng ShB (Fig. 1 *B*) or 0.1 ng Eag and 4 ng ShB (Fig. 1 *A*), the coexpressed current was greater than the single current. With 0.2 ng Eag and 8 ng ShB (Fig. 4 *C*, Fig. 6 *A*; cf. Chen et al., 1996), the coexpressed current was less than the single current. (Note that oocytes in Fig. 5 were selected for

similar peak transient currents to facilitate comparing kinetics in high Mg^{2+} experiments.)

An earlier study failed to show an interaction between Eag and ShB subunits (Tang et al., 1998). The present results suggest several factors to account for this. Their oocytes were tested 1–2 days after injection. Consistent with their results, we observed no interaction on days 1 and 2; however, interactions were clear by days 3 and 4, an expression period not tested in the other study. Immunocoprecipitation experiments in the earlier study (Tang et al., 1998) did not provide evidence for a physical interaction between subunit types, but these experiments also used preparations from early coinjected oocytes. (In our previous study, Chen et al., 1996, the same amount of Eag and ShB RNA was used as in Fig. 1 of this study, and observations were made between 3 and 6 days after injection. The source of the Eag message used in both studies (Chen et al., 1996; Tang et al., 1998) was identical, from Dr. G. Robertson; see Methods.) Moreover, Tang et al. (1998) injected equal, double, or triple amounts of Eag compared with ShB RNA. We previously showed that a low ratio of Eag RNA to ShB RNA is critical for detection of the interaction (Chen et al. 1996). To determine the decay kinetics of the transient current with confidence, it is important not to overexpress the delayed Eag component. An excess of Eag current expression can overwhelm the transient Sh-type current, making interactions extremely difficult to detect (Chen et al., 1996). This is especially important for later developmental stages because of the different developmental rate of Eag and Sh currents in the oocyte (Fig. 3). At 6 days the Eag current expression continued to grow at a high rate, whereas the Sh current expression saturated earlier. By using a lower ratio of Eag to Sh RNA, the transient component could be distinguished at later times after injection, when the interaction between subunit types becomes prominent.

Tang et al. (1998) suggested that the appearance of accelerated inactivation could come from clamping error due to large expressed currents. In this study we addressed this possibility in two ways. First, we examined oocytes in which current amplitudes were kept small, either by reducing voltage steps or by raising the holding potential to partially inactivate the transient current. In both cases the interaction could still be demonstrated. Second, in some analyses we compared oocytes that had similar current amplitudes. These comparisons showed that the influence of expression level and developmental time persists even when current amplitudes are matched between groups. Therefore, we conclude that series resistance and clamping error could not account for the interaction we have observed.

In the present study we have confirmed definite and reproducible interactions, and defined conditions in which those interactions can be seen. Two factors that are important are expression level and developmental time. This is consistent with the notion that heterologous expression of channel proteins in *Xenopus* oocytes is subject to cellular processes of protein synthesis, assembly, post-translational modifications, and surface targeting and clustering in the host cell (Papazian, 1999). Therefore, it is important to establish defined cellular conditions in which protein subunit interactions can be studied reproducibly, and to consider the cell biological mechanisms of oocytes when interpreting the results of heterologous channel expression.

We thank Dr. J. E. Engel for his comments on the manuscript. T. H. thanks the late A. T. Walker for electronic instrumentation.

This work was supported in part by National Institutes of Health grants to C.-F. W. and T. H.

REFERENCES

Aidley, D. J. 1998. Physiology of Excitable Cells, 4th Ed. Cambridge University Press, Cambridge.

Anderson, M. J., and M. W. Cohen. 1977. Nerve-induced and spontaneous redistribution of acetylcholine receptors on cultured muscle cells. *J. Physiol.* 268:757–773.

Barnard, E., P. Skolnick, H. Mohler, W. Sieghart, G. Biggio, C. Braestrup, A. N. Bateson, and S. Z. Langer. 1998. Subtypes of $GABA_A$ receptors: classification on basis of structure and receptor function. *Pharmacol. Rev.* 50:291–313.

Chen, M.-L., T. Hoshi, and C.-F. Wu. 1996. Heteromultimeric interactions among K^+ channel subunits from *Shaker* and *eag* families in *Xenopus* oocytes. *Neuron.* 17:535–542.

Covarrubias, M., A. A. Wei, and L. Salkoff. 1991. Shaker, Shal, Shab, and Shaw express independent K^+ current systems. *Neuron.* 7:763–773.

Frank, E., and G. D. Fischbach. 1979. Early events in neuromuscular junction formation in vitro. Introduction of acetylcholine receptor clusters in the postsynaptic membrane and morphology of newly formed synapses. *J. Cell Biol.* 83:143–158.

Ganetzky, B., G. A. Robertson, G. F. Wilson, M. C. Trudeau, and S. A. Titus. 1999. The Eag family of K^+ channels in *Drosophila* and mammals. *In* Molecular and Functional Diversity of Ion Channels and Receptors, Vol. 868. B. Rudy and P. Seeburg, editors. Annals of the New York Academy of Sciences. 356–369.

Guillemare, E., E. Honoré, L. Pradier, F. Lesage, H. Schweitz, B. Attali, J. Barhanin, and M. Lazdunski. 1992. Effects of the level of mRNA expression on biophysical properties, sensitivity to neurotoxins, and regulation of the brain delayed-rectifier K^+ channel Kv1.2. *Biochemistry.* 31:12463–12468.

Haugland, F. N., and C.-F. Wu. 1990. A voltage-clamp analysis of gene dosage effects of the *Shaker* locus on larval muscle potassium currents in *Drosophila. J. Neurosci*. 10:1357–1371.

Hille, B. 1992. Ionic Channels of Excitable Membranes, 2nd Ed. Sinauer Press, Sunderland, MA.

Honoré, E., B. Attali., G. Romey, F. Lesage, J. Barhanin, and M. Lazdunski. 1992. Different types of K^+ channel current are generated by different levels of a single mRNA. *EMBO J.* 11:2465–2471.

Hoshi, T., W. N. Zagotta, and R. W. Aldrich. 1991. Two types of inactivation in *Shaker* K^+ channels: effects of alterations in the carboxy-terminal region. *Neuron.* 7:547–556.

Isacoff, E. Y., N. Y. Jan, and L. Y. Jan. 1990. Evidence for the formation of heteromultimeric potassium channels in *Xenopus* oocytes. *Nature.* 345:530–534.

Iverson, L. E., M. A. Tanouye, H. A. Lester, and B. Rudy. 1988. A-type potassium channels expressed from the *Shaker* locus cDNA. *Proc. Natl. Acad. Sci. U.S.A.* 85:5723–5727.

Jan, L. Y., and Y. N. Jan. 1997. Cloned potassium channels from eukaryotes and prokaryotes. *Annu. Rev. Neurosci.* 20:91–123.

Kim, E., M. Niethammer, A. Rothschild, Y. N. Jan, and M. Sheng. 1995. Clustering of Shaker-type K^+ channels by interaction with a family of membrane-associated guanylate kinases. *Nature.* 378:85–88.

Li, M., Y. N. Jan, and L. Y. Jan. 1992. Specification of subunit assembly by the hydrophilic amino-terminal domain of the *Shaker* potassium channel. *Science.* 257:1225–1230.

Liu, F., Q. Wan., Z. P. Pristupa, X.-M. Yu, Y. T. Wang, and H. B. Niznik. 2000. Direct protein-protein coupling enables cross-talk between dopamine D5 and γ-aminobutyric acid A receptors. *Nature.* 403:274–280.

Ludwig, J., D. Owen, and O. Pongs. 1997. Carboxyl-terminal domain mediates assembly of the voltage-gated rat ether-à-go-go potassium channel. *EMBO J.* 16:6337–6345.

MacKinnon, R. 1991. Determination of the subunit stoichiometry of a voltage-activated potassium channel. *Nature*. 350:232–235.

McCormack, K., J. W. Lin, L. E. Iverson, and B. Rudy. 1990. *Shaker* K^+ channel subunits form heteromultimeric channels with novel functional properties. *Biochem. Biophys. Res. Commun.* 171:1361–1371.

Monyer, H., R. Sprengel, R. Schoepfer, A. Herb, M. Highchi, H. Lomeli, N. Burnashev, B. Sakmann, and P. H. Seeburg. 1992. Heteromeric NMDA receptors: molecular and functional distinction of subtypes. *Science.* 256:1217–1221.

Moran, O., W. Schreibmayer, L. Weigl, N. Dascal, and I. Lotan. 1992. Level of expression controls modes of gating of a K^+ channel. *FEBS Lett.* 302:21–25.

Niethammer, M., E. Kim, and M. Sheng. 1996. Interaction between the C terminus of NMDA receptor subunits and multiple members of the PSD-95 family of membrane-associated guanylate kinases. *J. Neurosci.* 16:2157–2163.

Papazian, D. M. 1999. Potassium channels: some assembly required. *Neuron.* 23:7–10.

Pardo, L., D. del Camino, A. Sánchez, F. Alves, A. Brüggemann, S. Beckh, and W. Stühmer. 1999. Oncogenic potential of EAG K^+ channels. *EMBO J.* 18:5540–5547.

Pongs, O., N. Kecskemethy, R. Müller, I. Krah-Jentgens, A. Baumann, H. H. Canal, S. Llamazares, and A. Ferrus. 1988. *Shaker* encodes a family of putative potassium channel proteins in the nervous system of *Drosophila. EMBO J.* 7:1087–1096.

Rudy, B. 1988. Diversity and ubiquity of K channels. *Neuroscience.* 25:729–749.

Rudy, B., and P. Seeburg. 1999. Molecular and Functional Diversity of Ion Channels and Receptors, Vol. 868. B. Rudy and P. Seeburg, editors. Annals of the New York Academy of Sciences.

Salkoff, L., and R. Wyman. 1981. Genetic modification of potassium channels in *Drosophila Shaker* mutants. *Nature.* 293:228–230.

Sanguinetti, M., C. Jiang, M. Curran, and M. Keating. 1995. A mechanistic link between an inherited and an acquired cardiac arrhythmia: *HERG* encodes the IKr potassium channel. *Cell.* 81:299–307.

Schwarz, T. L., B. L. Tempel, D. M. Papazian, N. Y. Jan, and L. Y. Jan. 1988. Multiple potassium-channel components are produced by alternative splicing at the *Shaker* locus in *Drosophila. Nature.* 331:137–142.

Sheng, M., J. Cummings, L. A. Roldan, Y. N. Jan, and L. Y. Jan. 1994. Changing subunit composition of heteromeric NMDA receptors during development of rat cortex. *Nature.* 368:144–147.

Silverman, S., P. Kofuji, D. Dougherty, N. Davidson, and H. Lester. 1996. A regenerative link in the ionic fluxes through the *weaver* potassium channel underlies the pathophysiology of the mutation. *Proc. Natl. Acad. Sci. U.S.A.* 93:15429–15434.

Singh, A., and S. Singh. 1999. Unmasking of a novel potassium current in *Drosophila* by a mutation and drugs. *J. Neurosci.* 19:6838–6843.

Taleb, O., and H. Betz. 1994. Expression of the human glycine receptor α1 subunit in *Xenopus* oocytes: apparent affinities of agonists increase at high receptor density. *EMBO J.* 13:1318–1324.

Tang, C.-Y., C. T. Schulteis, R. M. Jiménez, and D. M. Papazian. 1998. *Shaker* and *ether-à-go-go* K^+ channel subunits fail to coassemble in *Xenopus* oocytes. *Biophys. J.* 75:1263–1270.

Tejedor, F. J., A. Bokhari, O. Rogero, M. Gorczyca, J. Zhang, E. Kim, M. Sheng, and V. Budnik. 1997. Essential role for dlg in synaptic clustering of Shaker K^+ channel in vivo. *J. Neurosci.* 17:152–159.

Terlau, H., J. Ludwig, R. Steffan, O. Pong, and S. H. Heinemann. 1996. Extracellular Mg^{2+} regulates activation of rat *eag* potassium channel. *Pflugers Arch.* 432:301–312.

Timpe, L. C., Y. N. Jan, and L. Y. Jan. 1988. Four cDNA clones from the *Sh* locus of *Drosophila* induce kinetically distinct A-type potassium currents in *Xenopus* oocytes. *Neuron.* 1:659–667.

Wang, H., D. D. Kunkel, T. M. Martin, P. A. Schwartzkroin, and B. L. Tempel. 1993. Heteromultimeric K^+ channels in terminal and juxtaparanodal regions of neurons. *Nature.* 365:75–79.

Warmke, J., R. Drysdale, and B. Ganetzky. 1991. A distinct potassium channel polypeptide encoded by the *Drosophila eag* locus. *Science.* 252:1560–1562.

Wei, A., M. Covarrubias, A. Butler, K. Baker, M. Pak, and L. Salkoff. 1990. K^+ current diversity is produced by an extended gene family conserved in *Drosophila* and mouse. *Science.* 248:599–603.

Wu, C.-F., and M.-L. Chen. 1995. Coassembly of potassium channel subunits in *Drosophila*: the combinatorial hypothesis revisited. *Chin. J. Physiol.* 38:131–138.

Wu, C.-F., B. Ganetzky, F. N. Haugland, and A.-X. Liu. 1983. Potassium currents in *Drosophila*: different components affected by mutations of two genes. *Science.* 220:1076–1078.

Wu, C.-F., and B. Ganetzky. 1986. Gene and ionic channels in *Drosophila. In* Ion Channels in Neural Membranes. J. M. Ritchie, R. D. Keynes, and L. Bolis, editors. A. R. Liss, New York. 407–423.

Wu, C.-F., and B. Ganetzky. 1992. Neurogenetic studies of ion channels in *Drosophila. In* Ion Channels, Vol. 3. T. Narahashi, editor. Plenum Publishing Corp., New York. 261–314.

Wu, C.-F., and F. N. Haugland. 1985. Voltage clamp analysis of membrane currents in larval muscle fibers of *Drosophila*: alteration of potassium currents in *Shaker* mutants. *J. Neurosci.* 5:2626–2640.

Zerr, P., J. Adelman, and J. Maylie. 1998. Episodic ataxia mutations in Kv1.1 alter potassium channel function by dominant negative effects or haploinsufficiency. *J. Neurosci.* 18:2842–2848.

Zhong, Y., and C.-F. Wu. 1991. Alteration of four identified K^+ currents in *Drosophila* muscle by mutations in *eag. Science.* 252:1562–1564.

Zhong, Y., and C.-F. Wu. 1993. Modulation of different K^+ currents in *Drosophila*: a hypothetical role for the *eag* subunit in multimeric K^+ channels. *J. Neurosci.* 13:4669–4679.